REALIZATION OF A HIGH-DYNAMIC DISCRETE-TIME CONTROLLER FOR PWM INVERTER-FED INDUCTION MOTOR DRIVES

J. Böcker, J. Janning, K. Anbuhl

AEG Aktiengesellschaft, Institute of Drive Systems and Power Electronics, Germany

Abstract. This paper describes a controller of a PWM inverter-fed induction motor drive based on the well known principle of rotor flux orientation. A new aspect is the homogeneous discrete-time design of the complete control structure including measurement data acquisition and pulse width modulation. A discrete-time flux observer ensures accurate flux orientation even at standstill and additionally supplies one-step-ahead predicted current estimates, which compensates for computational delay. By these discrete-time considerations computing power can be saved whereas optimal control performance can be reached.
This control structure covers very different requirements of practical interest as smooth slow motion and operation at standstill as well as operations in the range of high flux weakening (up to ratios of 1:3...5 or more). In constant-flux range torque response times of about 5 ms are reached. Even at a flux weakening ratio of up to 1:3.5 a torque response time of 15...20 ms was measured.
The controller has been successfully proved in several drives up to a power of 960 kW. In all operation modes the control characteristics are comparable with those of DC drives.

Keywords. Induction motor, discrete-time controller, flux observer, current prediction, flux weakening, high-dynamic current control, standstill operation.

INTRODUCTION

The principle of flux-oriented control of induction motors is well known from numerous publications. Nowadays drive controllers are usually realized as sampling microprocessor systems. For this a discrete-time controller design is suitable. Controllers designed by discrete-time considerations are no more complicated than quasi-continuous controllers, but they save computing power and are able to realize step response times of a few sampling periods. One new aspect of this paper is the consistent application of discrete-time control design methods including data acquisition and pulse width modulation.

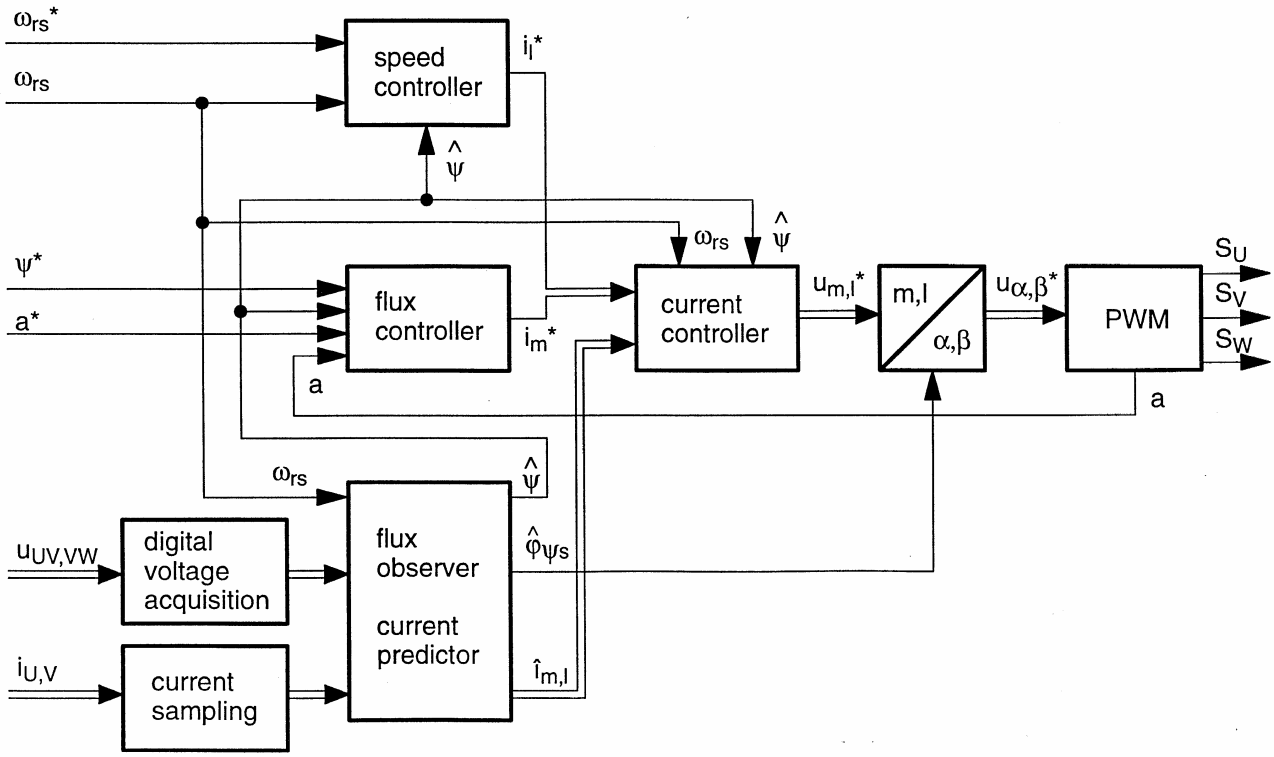

Figure 1: Control structure

FLUX OBSERVER

The control structure is depicted in fig. 1. Because the rotor flux is not measurable, an observer is used to calculate estimates of the rotor flux from measurable data, i.e. from stator phase currents i_u, i_v, voltages u_{uv}, u_{vw} and rotor speed ω_{rs}. The estimated flux angle $\hat{\varphi}_{\psi s}$ is needed to realize flux-oriented control. The absolute rotor flux estimate $\hat{\psi}$ is used by the flux controller.

The Luenberger-type observer consists of a discrete-time model of the induction motor and a feedback of the observation error, cf. Böcker and Janning [1], Böcker [2]. The observer operates as one-step-ahead predictor. Because a full-order observer is used, it is able to supply predicted values $\hat{i}_m, \hat{i}_l$ of the flux-oriented current components, which compensates for computational delays of the control algorithm.

Practical results have shown that the observer ensures accurate flux orientation even at low speed and standstill. Fig. 2 shows the control performance at 1 ‰ rated speed and 50 % rated load current. Remarkable is the sinusoidal phase current i_u and the corresponding constant load current i_l which enables a smooth rotational motion.

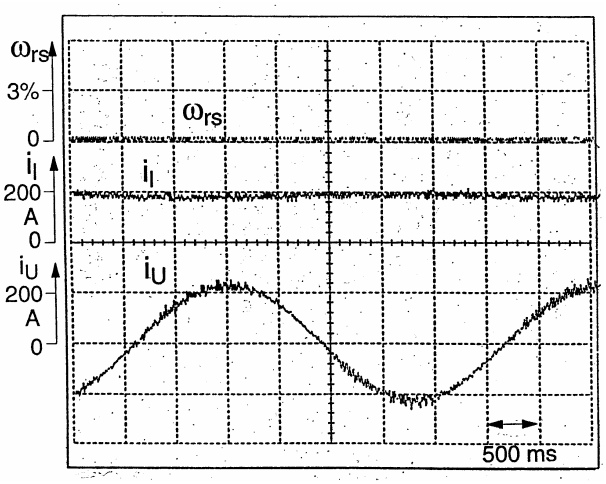

Figure 2: Motion at 1 ‰ rated speed under load

CURRENT CONTROLLER

The structure of the current controller depicted in fig. 3 consists of EMF compensation, feedforward and PI-type feedback block. The controller is designed by a decoupling condition regarding the closed-loop behaviour of magnetizing and load current components i_m, i_l. The closed-loop dynamics are determined by discrete-time pole placement, which includes the possibility of dead-

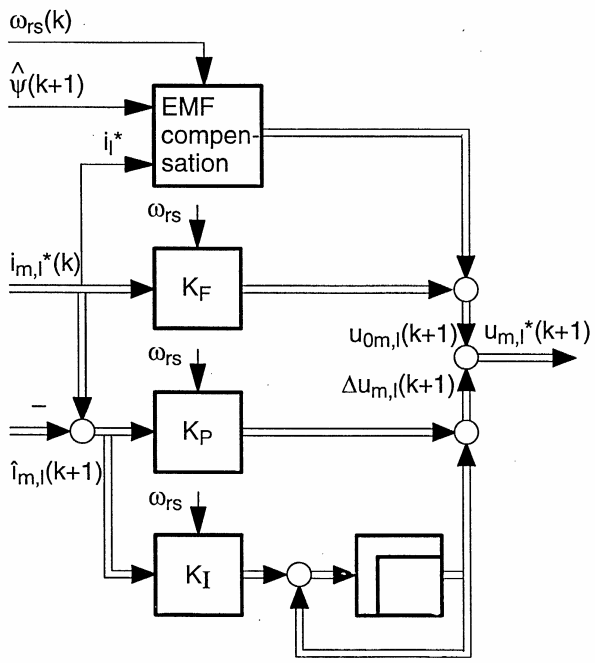

Figure 3: Current controller

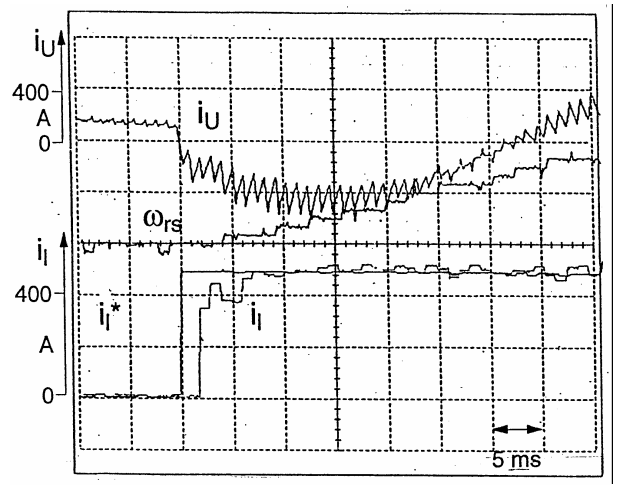

Figure 4: Step response of load current at 35 % rated speed

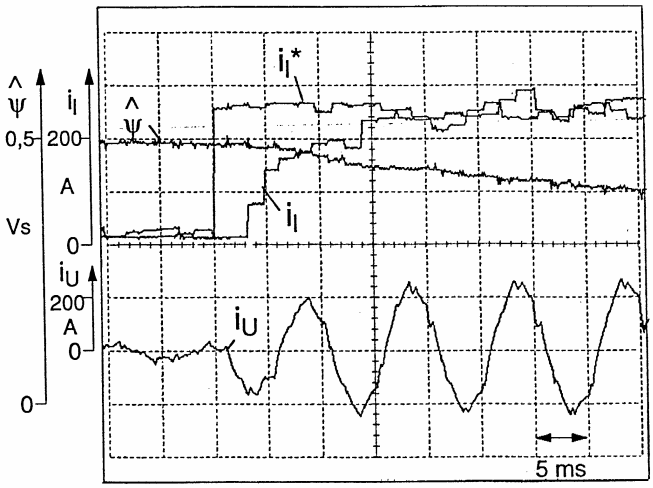

Figure 5: Step response of load current at 340 % rated speed

beat design. A suitable placement of poles is in the range of 0.2...0.3, i.e. a control error is reduced every control cycle to 20...30 % of its previous value.

Fig. 4 and 5 show step responses of the load current i_l, in constant-flux and flux weakening ranges using an 160 kW induction motor. The current rise time is about 5 ms in constant-flux range. In flux weakening range the rise time is still about 10 ms up to 1:2 flux weakening ratio and 15...20 ms up to 1:3.5 flux weakening ratio (cf. fig. 5).

FLUX CONTROLLER

The flux controller governs the flux by imposing a suitable reference of the magnetizing current component i_m*. Usually the flux reference value ψ* is kept constant as long as the inverter voltage is sufficient. With increasing speed the voltage reaches its maximum. Hence, the flux has to be reduced for higher speeds (flux weakening range). A common method for flux weakening is reducing the flux reference value depending on the fundamental frequency.

Here flux reduction is achieved indirectly by controlling the modulation index a of the pulse width modulator as depicted in fig. 6. By this approach, flux dependence on non-constant DC link voltage and leakage voltage drop in flux weakening range is implicitly considered.

The control of the modulation index a is not carried out as an additional cascaded outer control loop because it is not appropriate for quick dynamic speed operations, which require fast flux reduction. Therefore the reference value i_m* is directly used for controlling a. To ensure constant gain of the control loop for varying speed, the actual flux estimate 'if is used for controller gain adaption. Switching over between modes of constant-flux and constant-modulation-index control is simply realized by minimum selection.

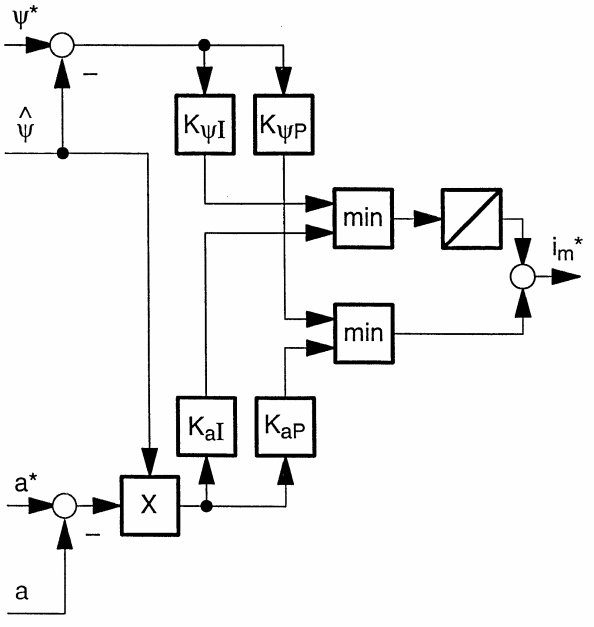

Figure 6: Flux controller

PERFORMANCE AT HIGH FLUX WEAKENING

A load current step response at 340% rated speed has been already shown in fig. 5. To keep the modulation index constant at this operation, the flux has to decrease because of increasing leakage voltage drop and load-dependent DC link voltage. By reason of flux decrease with increasing load current, torque cannot exceed a maximum, since it is determined by the product of load current and rotor flux. To avoid demagnetizing with too large load current references, it is necessary to limit the load current demand when the torque reaches its maximum.

In fig. 7 a trapezoidal torque reference exceeding the maximal torque is shown at 340% rated speed. The estimated torque $\hat{T}$ (which is calculated from $\hat{i}_l$ and $\hat{\psi}$) reaches its maximal possible value, while the flux $\hat{\psi}$ remains constant.

Behaviour in motor and generator operation modes are similar. However, generatoric maximal torque and flux values are absolutely greater than the motoric ones. The reason is a higher DC link voltage in generator operation mode, which enables a greater motor voltage with constant modulation index.

A dynamic flux reduction and flux rising, respectively, can be seen from the fast speed reversal from -300 % to +300 % rated speed in fig. 8. While the motor decelerates, the rotor flux $\hat{\psi}$ is simultaneously risen by an enhanced magnetizing current component $\hat{i}_m$. When the flux reaches its reference value, the flux controller changes over from constant-modulation-index control to constant-flux control mode whereafter the modulation

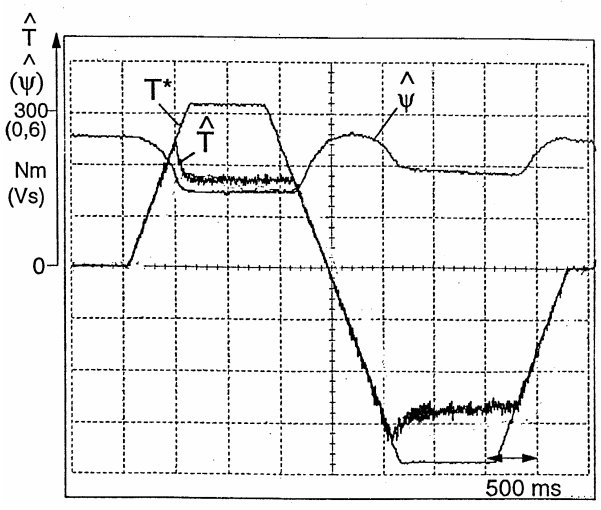

Figure 7: Torque demands at 340 % rated speed

index *a* decreases. After speed has reversed, *a* increases again and reaches its reference value. Dynamic flux reduction is now performed by a negative magnetizing current component $\hat{i}_m$.

Flux weakening has been proved up to a ratio of 1:3.5, so far. Nevertheless, flux weakening' ratios of 1:5 or more can be expected.

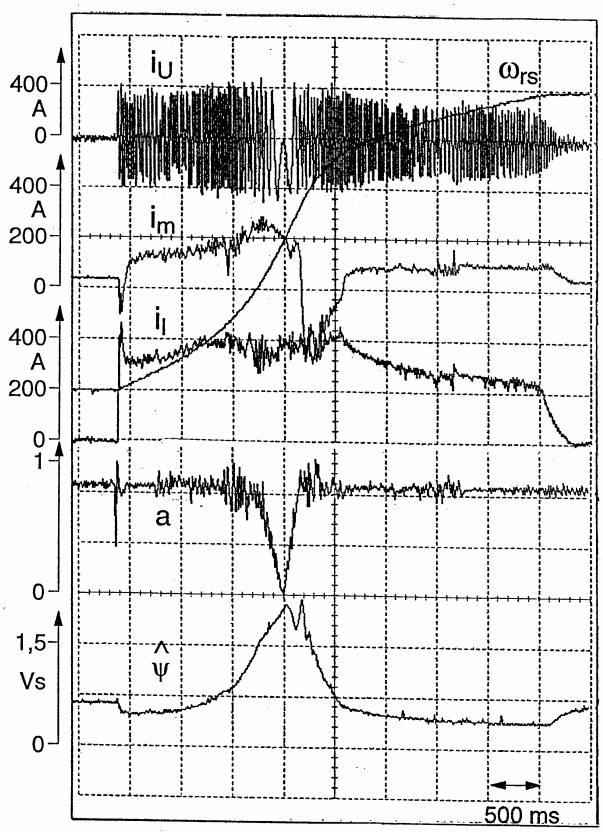

Figure 8: Speed reversal from -300 % to 300 % rated speed

PWM AND SAMPLING STRATEGY

Inverter switching times are calculated each sampling period depending on the actual voltage reference value by using vector modulation method for pulse width modulation (cf. fig. 1). Control algorithm and pulse generation are strictly synchronized using the vector modulation periods as sampling periods of measurement data acquisition and control loops. A higher controller sampling rate is not appropriate because the inverter cannot react on additional voltage demands. By such a synchronization of pulse generation, data acquisition and control an optimal control performance can be achieved.

Since synchronized pulse patterns are used for GTO inverters for higher fundamental frequencies, sampling periods now have to vary with the fundamental frequency. However, the truly discrete-time design of flux observer and current controller facilitates the handling of varying sampling periods.

Fig. 9 shows the sampling frequency f_A in dependence on the fundamental frequency f_S. In the range of synchronous pulsing n_A specifies the ratio of the sampling frequency f_A to the fundamental frequency f_S while n_p is ratio of the pulse frequency to f_S The maximal fundamental frequency f_S is either limited by the maximal pulse frequency of the GTO modules or by the maximal sampling frequency f_A of the microprocessor realization. The control structure itself sets no limits to the fundamental frequency.

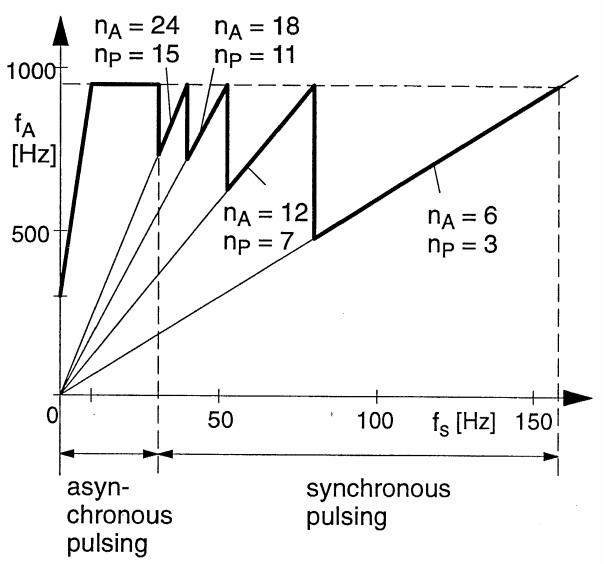

Figure 9: Sampling frequency f_A versus fundamental frequency f_S

MICROPROCESSOR REALIZATION

The control structure was implemented in C programming language on a multi microprocessor system. The tasks of flux observation, current control and pulse width modulation have to be sequentially processed every sampling period and consume the main computing power. None of these tasks contain structures suitable for parallel processing. Therefore these tasks are placed on one microprocessor whose computing power limits the maximal sampling frequency f_A. Another microprocessor serves flux control, speed control and communication interface tasks.

With this microprocessor realization measurement data sampled at the last instant can be processed within the actual sampling period and influence the firing pulses after a computational delay of one period. The sampling period varies in the range of 1 to 2.5 ms.

INDUSTRIAL APPLICATIONS

The controller has been successfully proved in several drives up to a power of 960 kW. The high performance of the controller even at high flux weakening opens up many possible applications. Potential applications are high performance drives in steel and paper mills (Fuchs [3]), traction drives, test stand drives for combustion engines and gears.

CONCLUSIONS

The proposed control structure

- uses a flux observer to ensure accurate flux orientation even at stand still
- compensates for computational delays by one-step-ahead current prediction
- realizes torque step response time about 5 ms in constant-flux range
- still realizes torque step response times of about 10 ms up to 1:2 flux weakening ratio and of 15...20 ms up to 1:3.5 flux weakening ratio
- enables dynamic flux weakening and flux rising for fast accelerations and decelerations, respectively
- has been successfully proved in several drives up to a power of 960 kW
- is applicable for drives in steel and paper mills as well as for test stand drives

It has been shown that accurate results are achieved by the homogeneous discrete-time design of the complete control structure, which is suitable for microprocessor realizations. Quasi-continuous approaches should be obsolete.

REFERENCES

1. Böcker, J., Janning, J., 1991: Discrete-Time Flux Observer for PWM Inverter-Fed Induction Motors. EPE'91, vol. 2, 171-176

2. Böcker, J., 1990: Discrete-Time Model of an Induction Motor. ETEP, 1, no. 2, 65-71

3. Fuchs, F. W., 1993: Standard-Umrichterantriebe im Einsatz bei verschiedensten Produktionsprozessen. ETG-Fachbericht 42, 131-139, VDE-Verlag, Berlin